Heme Pocket Disorder in Myoglobin: Reversal by Acid-Induced Soft Refolding†

Maria C. Piro,‡,§ Valeria Militello,|| Maurizio Leone,⊥ Zigmunt Gryczynski,‡,# Stanley V. Smith,▽ William S. Brinigar,▼ Antonio Cupane,*,⊥ Fred K. Friedman,*,▽ and Clara Fronticelli*,‡,◆

Department of Biochemistry and Molecular Biology, University of Maryland Medical School, Baltimore, Maryland 21201, Istituto Nazionale di Struttura della Materia and Istituto di Fisiologia Umana, Universita di Palermo, 90123 Palermo, Italy, Istituto Nazionale di Struttura della Materia and Dipartimento di Scienze Fisiche ed Astronomiche, Universita di Palermo, 90123 Palermo, Italy, Center for Fluorescence Spectroscopy, University of Maryland Medical School, Baltimore, Maryland 21201, Laboratory of Metabolism, Center for Cancer Research, National Cancer Institute, Bethesda, Maryland 20892, Department of Chemistry, Temple University, Philadelphia, Pennsylvania 19122, and Department of Anesthesiology, Johns Hopkins University School of Medicine, Baltimore, Maryland 21287

Received April 2, 2001; Revised Manuscript Received June 18, 2001

ABSTRACT: The protein folding process of heme proteins entails generation of not only a correct global polypeptide structure, but also a correct, functionally competent heme environment. We employed a variety of spectroscopic approaches to probe the structure and dynamics of the heme pocket of a recombinant sperm whale myoglobin. The conformational characteristics were examined by circular dichroism, time-resolved fluorescence spectroscopy, FTIR spectroscopy, and optical absorption spectroscopy in the temperature range 300−20 K. Each of these spectroscopic probes detected modifications confined exclusively to the heme pocket of the expressed myoglobin relative to the native protein. The functional properties were examined by measuring the kinetics of CO binding after flash-photolysis. The kinetics of the expressed myoglobin were more heterogeneous than those of the native protein. Mild acid exposure of the ferric derivative of the recombinant protein resulted in a protein with "nativelike" spectroscopic properties and homogeneous CO binding kinetics. The heme pocket modifications observed in this recombinant myoglobin do not derive from inverted heme. In contrast, when native apomyoglobin is reconstituted with the heme in vitro, the heme pocket disorder could be attributed exclusively to 180° rotation of the bound heme [La Mar, G. N., Toi, H., and Krishnamoorthi, R. (1984) *J. Am. Chem. Soc. 106*, 6395−6401; Light, W. R., Rohlfs, R. J., Palmer, G., and Olson, J. S. (1987) *J. Biol. Chem. 262*, 46−52]. We conclude that exposure to low pH decreases the affinity of globin for the heme and allows an extended conformational sampling or "soft refolding" to a nativelike conformation.

The various families of heme proteins play critical roles in numerous biological processes, particularly those involving electron transfer and oxygen transport. While the common reaction center for these processes is the heme moiety, the unique function of each heme protein is governed by a complex interplay of forces that dictate protein folding and the protein−heme interaction (*1*−*5*). The oxygen carrriers myoglobin and hemoglobin have long served as model heme proteins to elucidate these fundamental interactions that link structure and function (*6*−*10*). Recombinant DNA techniques have been increasingly applied to biophysical studies of these heme proteins. Thus, site-directed mutagenesis of myoglobin (*11*−*15*) and hemoglobin (*16*−*21*) was used to introduce desired and defined perturbations into the native proteins and thus address questions such as the role of cavities, steric hindrance, electrostatic interactions, and hydrogen bonding in the regulation of protein dynamics and ligand affinity. However, a potential question when using recombinant proteins is whether correct, nativelike, protein folding occurs. For heme proteins this problem is compounded by additional apoprotein−heme interactions, and the role of heme in directing the final folding of the native protein (*22*−*25*). The spectral properties of the heme have proven particularly advantageous in heme protein structure−function studies, since these provide an internal, native probe of the reaction center that reflects subtle structural features of heme and its environment. In this study, we applied a variety of spectroscopic probes of heme structure and dynamics to examine the role of the heme in protein folding of sperm whale

† This work has been supported by Italian National Council Grant 97.04350 (to A.C. and C.F.), U.S. Public Health Service, National Institutes of Health (NIH), Grant PO1 HL48517, the Eugene and Mary B. Meyer Center for Advanced Transfusion Practice and Blood Research (to C.F.), and the NIH National Center for Research Resources Grant RR-0811 (to Z.G.).

* To whom correspondence should be addressed. A.C.: Istituto Nazionale di Struttura della Materia and Dipartimento di Scienze Fisiche ed Astronomiche, Universita di Palermo, Via Archirafi 36, 90123 Palermo, Italy; Telephone (39-091)6234220, Fax (39-091)616-2461, E-mail cupane@fisica.unipa.it. F.K.F.: National Cancer Institute, Building 37, Room 3E24, Bethesda, MD 20892; Telephone (301) 496-6365, Fax (301) 496-8419, E-mail fkfried@helix.nih.gov. C.F.: Department of Anesthesiology, Johns Hopkins University School of Medicine, 600 N.Wolfe St., Blalock Building, Room 1414, Baltimore, MD 21287; Telephone (410) 614-9420, Fax (410) 955-7165, E-mail cfrontic@jhmi.edu.

‡ Department of Biochemistry and Molecular Biology, University of Maryland Medical School.

§ Present address: Department of Experimental Medicine and Biochemical Science, Università Tor Vergata, 00133 Rome, Italy.

|| Istituto Nazionale di Struttura della Materia and Istituto di Fisiologia Umana, Universita di Palermo.

⊥ Istituto Nazionale di Struttura della Materia and Dipartimento di Scienze Fisiche ed Astronomiche, Universita di Palermo.

Center for Fluorescence Spectroscopy, University of Maryland Medical School.

▽ Laboratory of Metabolism, Center for Cancer Research.

▼ Department of Chemistry, Temple University.

◆ Department of Anesthesiology, Johns Hopkins University School of Medicine.

10.1021/bi010652f CCC: $20.00
Published on Web 09/05/2001

myoglobin. We first found evidence of aberrant heme pocket folding in recombinant myoglobin expressed in *Escherichia coli*, via a modified expression system. This partially incorrect folding was accompanied by pronounced conformational heterogeneity, as reflected by the spectroscopic properties of the protein and kinetics of CO binding. We furthermore found that incubation of the recombinant ferric myoglobin at slightly acid pH reduced this heterogeneity and restored nativelike spectroscopic properties and CO binding kinetics. These results provide new insights on the relationship between the rate of protein synthesis, heme pocket refolding, and heme binding. In the absence of a correct synchrony between these events, the conformation of the heme pocket is trapped in a metastable state that prevents the attainment of the final, correctly folded state.

EXPERIMENTAL PROCEDURES

Plasmid Construction. The initial objective was to construct a plasmid which would direct the synthesis of sperm whale myoglobin with a native sequence, i.e., with the N-terminal Met removed. First pAltMb was constructed by inserting the 500 bp fragment from between the *Pst*I and *Kpn*I sites of pMb413 into pAlter (Promega) which had been digested with the same two endonucleases. The insert contained the entire synthetic Mb[1] gene constructed by Springer and Sligar (*26*). The Mb gene was then modified at three sites using the pAlter mutagenesis system of Promega. Mutagenic deoxyoligonucleotides were synthesized by DNAgency (Malvern, PA). The first modification was to introduce a *Nde*I site at the initiation Met codon by changing the sequence from ACAATG to CATATG. An additional modification was to remove the *Hin*dIII site in the vicinity of the Lys56 codon, and to replace the *Sac*I site adjacent to the *Kpn*I site with a *Hin*dIII site. The sequence at the Lys56 codon was changed from AAAGCTT to AAGGCTT so no change in the protein sequence resulted. The modified plasmid is designated pAltMbNdH and was used to generate the 489 bp Mb insert by digestion with *Nde*I and *Hin*dIII.

The vector was prepared from pHE2 (*27*). This plasmid contains genes for *Escherichia coli* methionine aminopeptidase (MAP) as well as the α- and β-globins. It contains two *Hin*dIII sites, one at the 3′-end of the β-globin gene and the other at the 3′-end of the MAP gene. To facilitate replacement of the α- and β-globin genes with the Mb gene, the *Hin*dIII site at the end of the MAP gene was eliminated by changing the sequence from TAAGCTT to TAATAAT, thereby introducing a second stop codon. This plasmid is designed pHbA1. To generate the vector, pHbA1 was exhaustively digested with *Hin*dIII followed by partial *Nde*I digestion. There are three *Nde*I sites in pHbA1. Hydrolysis at only the *Nde*I site at the beginning of the α-globin gene gives a 5900 bp fragment. This fragment was isolated by gel electrophoresis and ligated to the 489 bp fragment obtained from pAltMbNdH. The resulting plasmid contains both the MAP gene as well as the Mb gene, and is designated pCHMb. The Mb gene was sequenced by the DNA Sequencing Facility at the University of Pennsylvania, using a primer which annealed approximately 60 residues from the initiation ATG codon. Although Mb expression was good, HPLC analysis and Edman sequencing revealed that the MAP could remove up to seven amino-terminal residues from the recombinant Mb. Thus, the following growth conditions were developed in order to minimize processing of the N-terminal residues.

Protein Expression and Purification. E. coli strain JM109 containing the pCHMb plasmid was grown at 30 °C in 5 L of TB medium containing 50 μg/mL ampicillin, to an absorbance of 0.3 OD at 600 nm. Induction was accomplished by adding isopropyl-β-D-thiogalactopyranoside to a final concentration of 0.2 mM. The culture was supplemented with hemin (10 mg/L) and glucose (10 g/L). Cells were then incubated at 30 °C for 4 h, harvested by centrifugation, and frozen at −80 °C. After thawing, the reddish bacteria pellets were resuspended in 50 mM Tris, pH 8.0 (4 mL per gram of wet cells), and subjected to 4 freeze/thaw cycles. Lysozyme (1 mg/mL), DNase (5 μg/mL), dithiothreitol (0.5 mM), and benzamidine (1 mM) were then added to the homogenized cells and left overnight at 4 °C. The suspension was sonicated for 4 min at medium intensity, on ice, and then centrifuged to remove cell debris. Pellets were resuspended in 50 mL of 1 mM benzamidine, 50 mM Tris (pH 8.0), sonicated, and centrifuged as above. At this point, the two supernatants were combined, and the pH was adjusted to 6.0 with 0.4 M monobasic phosphate buffer and dialyzed overnight against 1 mM benzamidine, 0.01 M phosphate buffer (pH 6.0). Purification was performed on a CM 52 column (1.5 × 15 cm) using a gradient from 0.01 M phosphate buffer at pH 6.0 to 0.05 M dibasic phosphate and a flow rate of 0.6 mL/min for 50 min. The resulting recombinant myoglobin was at least 95% pure by SDS−PAGE analysis and reverse-phase HPLC. Amino acid sequencing indicated that the purified Mb retained the methionine initiator. Spectroscopic measurements did not detect formation of sulfmyoglobin. Material prepared by this procedure is termed untreated recombinant myoglobin (u-Mb).

Acidic Oxidation−Reduction Treatment for Heme Pocket Refolding. This procedure follows that described by Shen et al. (*27*). To u-Mb in 20 mM phosphate at pH 5.3 was added $K_3Fe[CN]_6$ in a molar ratio 1:1.2, and this solution was incubated at 4 °C for 48 h. The ferricyanide was removed and simultaneously the protein converted to the CO form by filtration through a CO-saturated Sephadex G15 column that was preequilibrated with 20 mM phosphate (pH 7.5), in which a small amount of a saturated dithionite solution had been absorbed on the top. This additional step yields the treated recombinant Mb (t-Mb).

CD Spectroscopy. The CD spectra were recorded at 15 °C in 20 mM phosphate buffer (pH 7.4) on an AVIV CD 60 spectropolarimeter (Aviv Associates, Lakewood NJ). Each spectrum represents the average of five scans. For the deoxy derivatives, the samples were equilibrated with nitrogen and transferred anaerobically into a 1 cm rubber-capped cuvette, and 5 μL of a solution containing 200 mg/mL dithionite was injected with a needle through the rubber cap. The carbonmonoxy derivatives were obtained by flushing the cuvette containing the deoxy sample with CO through needles inserted in the cuvette rubber cap. The helical content was

[1] Abbreviations: Mb, native sperm whale myoglobin; u-Mb, untreated recombinant myoglobin; t-Mb, recombinant myoglobin after acidic oxidation−reduction treatment; MAP, methionine aminopeptidase; MEM, maximum entropy method.

estimated on the basis of CD spectra between 250 and 220 nm, at 15 °C (after dithionite removal through gel filtration).

The denaturation temperature, T_m, was determined for the carbonmonoxy derivative at 225 nm in 20 mM phosphate buffer (pH 7.4) with constant stirring. The data were collected between 56 and 85 °C at 2 °C intervals with an average time of 10 s at each temperature. The temperature inside the spectrophotometric cuvette was controlled to an accuracy of 0.1 °C.

Fluorescence Spectroscopy. Fluorescence lifetime measurements were carried out using a frequency domain 10 GHz fluorometer equipped with a Hamamatsu 6 μm microchannel plate detector (*28*). The instrument covers a wide frequency range between 11 and 5000 MHz, which allowed detection of lifetimes ranging from several nanoseconds to a few picoseconds. Samples were placed in a "shielded cuvette" of 1 cm path length (*29*−*31*). Sample emission was filtered through an Oriel interference filter centered at 340 nm and a Corning 7-60 broad band filter. For reference, we used the scatter of the sample solution filtered through an Oriel interference filter at 289 nm and neutral density filters. All filters were calibrated to obtain identical optical path lengths at 294 and 340 nm. The measurements were carried out at room temperature. Time-resolved intensity data were analyzed using the sum of discrete exponentials:

$$I(t) = I_0 \sum_i a_i e^{t/\tau_i} \qquad (1)$$

where a_i is the amplitude and τ_i is the lifetime of the ith discrete component. Lifetimes and amplitude were recovered by nonlinear least-squares analysis.

FTIR Spectroscopy. FTIR spectra were measured at room temperature using a Bio-Rad FTS-40A FTIR spectrophotometer equipped with a PbS detector. Samples in the carbonmonoxy form, at a final concentration of about 7 mM, were placed in a Specac cell with CaF_2 windows and a 0.05 mm spacer. Spectra in the range 1900−2000 cm^{-1} were registered with 256 scans at 2 cm^{-1} resolution. Baseline correction was performed by subtracting the solvent + cell spectrum, after appropriate normalization. Spectral analysis in terms of Voigtian components was performed with the program Peakfit (SPSS Science, Chicago, IL).

Low-Temperature Optical Absorption Spectroscopy. Absorption spectra in the region 500−350 nm and in the temperature range 300−20 K were recorded in digitized form at 0.5 nm intervals with a Cary Varian 2300 spectrophotometer set at 0.5 nm/s scan speed, 1s integration time, and 0.5 nm bandwidth; under these conditions, the spectral resolution was about 20 cm^{-1} at 420 nm. The proteins were diluted to a final concentration of about 10^{-5} in heme, in 65% v/v glycerol−water solutions containing 0.1 M phosphate buffer (pH 7.0 in water, at room temperature) and 3 $\times$ 10^{-4} M sodium dithionite, to yield homogeneous and transparent samples at all temperatures.

The spectra were analyzed using an approach previously described in detail (*32*). The absorption profile is modeled as a convolution of three terms:

$$A(\nu) = M\nu[L(\nu) \otimes G(\nu) \otimes P(\nu)] \qquad (2)$$

where M is a constant proportional to the square of the electronic dipole transition moment, ν denotes the frequency, and $\otimes$ indicates the convolution operator. The first term, $L(\nu)$, is a sum over all Lorentzian lines arising from the coupling of the electronic transition to the high-frequency vibrational modes of the system according to the Franck−Condon principle. The second term, $G(\nu)$, takes into account the coupling of the electronic transition to a bath of low-frequency modes of the system: it can be shown that such a coupling yields a Gaussian distribution of fundamental frequency (i.e., brings about the convolution with a Gaussian line shape) (*33*). The third term, $P(\nu)$, takes into account further contributions to the line shape arising from inhomogeneous effects such as different conformational substates and heme environments (*33*). Detailed mathematical expressions for the three terms have been previously presented (*17*, *18*) and are, therefore, not reported here.

Information on the local dynamic properties of the system (heme + ligand + heme pocket) is obtained through the temperature dependence of parameters $\sigma^2(T)$ and $\nu_0(T)$, i.e., of the Gaussian line width and of the peak frequency of the band, which, within the harmonic Einstein approximation, is given by

$$\sigma^2_{\text{Harm}}(T) = NS\langle\nu\rangle^2 \coth[h\langle\nu\rangle/2k_BT] + \sigma_{in}{}^2 \qquad (3)$$

$$\nu_{0\,\text{Harm}}(T) = \nu_{00} - (1/4)N(1-R)\langle\nu\rangle \coth[h\langle\nu\rangle/2k_BT] \qquad (4)$$

where N is the number of soft modes and S and R are the average linear and quadratic coupling constants, respectively; the term $\sigma_{in}{}^2$ takes into account the temperature-independent contributions to the line width arising from spectral and conformational heterogeneity, while the term ν_{00} contains temperature-independent contributions to the peak position of the band arising, e.g., from the local electric field experienced by the chromophore. The subscripts "Harm" indicate that eqs 3 and 4 are valid only in the harmonic regime: deviations of the σ^2 temperature dependence from eq 3 are therefore indicative of the onset of nonharmonic motions in the system.

CO Binding Kinetics. Flash photolysis was carried out in solutions containing 5 μM heme and 50 μM CO at 20 °C in 0.1 M Bis-Tris (pH 7.0) containing 0.1 M KCl. Approximately 0.5 mg of sodium dithionite was added to reduce any ferric heme to the ferrous state. The instrumentation and experimental details for laser flash photolysis were essentially as previously described (*34*). The apparatus was constructed in conjunction with the Biomedical Instrumentation and Engineering Program of the National Instititutes of Health. The signal acquisition and processing system was designed to minimize hardware filtering that would distort the data and subsequent kinetic analysis. Instrument performance was previously validated in numerous studies using cytochrome P450 (*35*−*41*) and hemoglobin (*17*, *42*). The experimental procedure entailed generation of a pulse (0.6 μs) from a dye laser to disrupt the photolabile heme Fe−CO bond. The recombination of CO with the heme protein was then monitored by following the absorbance change at 436 nm, with the data transmitted to a microcomputer for processing and analysis. Standard multiexponential analysis of the kinetic data was performed according to

$$\Delta A(t) = \sum_{i=1}^{n} a_i e^{(-k_i t)} \quad (5)$$

where $\Delta A(t)$ is the total absorbance change observed at time t, a_i is the absorbance change for component i at $t = 0$, k_i is the observed pseudo-first-order rate constant for component i, and n is the number of independent components. Least-squares analysis was performed with RS/1 software (BBN Software Products, Cambridge, MA) on a Dell microcomputer.

Maximum entropy method (MEM) analysis was performed on the kinetic traces using the MEMSYS 5 software package with a flash photolysis specific interface (Maximum Entropy Data Consultants, Ltd., Suffolk, U.K.). Normalized data were subjected to MEM analysis using 200 decay bins while searching from 1 to 1000 in log k space.

Materials. Sperm whale myoglobin was obtained from Sigma (prior to the ban on whale products) and used without further purification. All chemicals were of the highest reagent grade.

RESULTS

Circular Dichroism. Room temperature CD spectra of the Soret region are shown in Figure 1A and 1B for the deoxy and carbonmonoxy derivatives, respectively. For both derivatives, the CD signal of the recombinant untreated protein (u-Mb) is characterized by a lower intensity and greater line width than native Mb and t-Mb. The CD signal was completely restored after the acidic oxidation−reduction treatment described under Experimental Procedures.

CD measurements in the far-UV region of the spectrum indicated that Mb, u-Mb, and t-Mb have the same helical content (data not shown). The CD at 225 nm was measured at different temperatures to determine the relative thermal stabilities of u-Mb and t-Mb. Figure 2 shows a second-derivative plot of the thermal denaturation of the carbonmonoxy derivatives of u-Mb and t-Mb, in which the zero point on the y axis corresponds to the melting temperature (T_m). The results indicate that both proteins have a similar stability to thermal denaturation with T_m values of 74.3 and 74.5 °C for u-Mb and t-Mb, respectively.

Fluorescence Lifetime Measurements. The lower Soret CD of u-Mb could have arisen from inverted heme, which results from heme insertion into its pocket in either of two orientations that differ by a 180° rotation about the $\alpha-\gamma$ meso axis (*43*, *44*). We examined this possibility by measuring the fluorescence lifetimes of tryptophans in positions 7 and 14 of u-Mb and t-Mb. The experimental values are listed in Table 1. Four discrete lifetimes can be resolved along with amplitudes that reflect the relative amount of each component. We attribute the shorter components, τ_1 and τ_2, at 25 and 129 ps, to the tryptophans in positions 14 and 7, respectively, in which the heme is correctly positioned in the heme pocket. These results agree fairly well with the values of 36 and 114 ps calculated on the basis of the atomic coordinates for myoglobin with the "normal" configuration of the heme (*45*, *46*). The longer lifetime component τ_3 at 1504 ps is predicted for both Trp14 and Trp7 in the presence of 180° inverted hemes. The data show that the amount of 180° inverted heme is only 2% in u-Mb and 1% in t-Mb. This minute fraction of inverted heme cannot be responsible for the large modification of the Soret CD spectrum observed in u-Mb. It is important to stress that the very small difference in the amplitude of the third lifetime component τ_3 for u-Mb and t-Mb can be recovered with very good confidence due to its significant contribution to the steady-state intensity. For comparison, in Table 1 we present the fractional intensities. For lifetime component τ_3, the small change in amplitude corresponds to a significant fractional intensity change (from 20.4% to 11.7%). The fourth com-

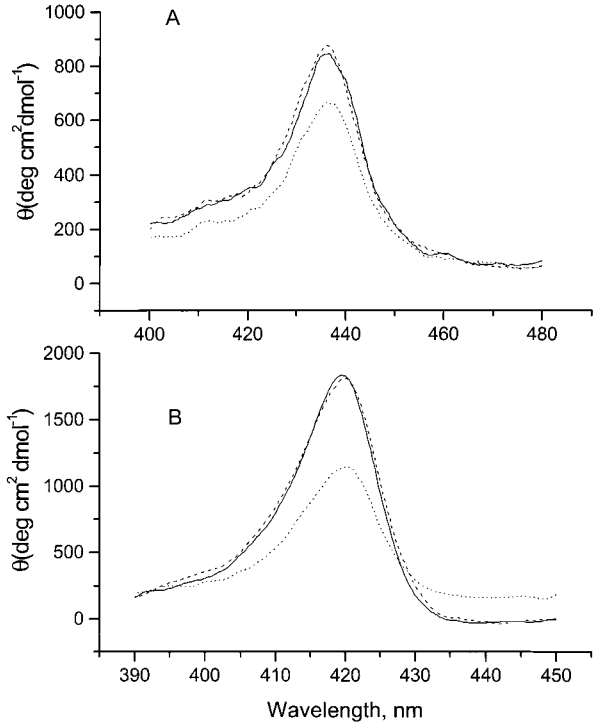

FIGURE 1: CD spectra of deoxy (A) and carbonmonoxy (B) myoglobins. Soret region spectra are shown for native sperm whale myoglobin (—), recombinant untreated myoglobin (u-Mb) prior to the acidic oxidation−reduction treatment (···), and recombinant treated myoglobin (t-Mb) after the acidic oxidation−reduction treatment (− −). Protein concentration was 5×10^{-6} M in 20 mM phosphate buffer (pH 7.4) at 15 °C.

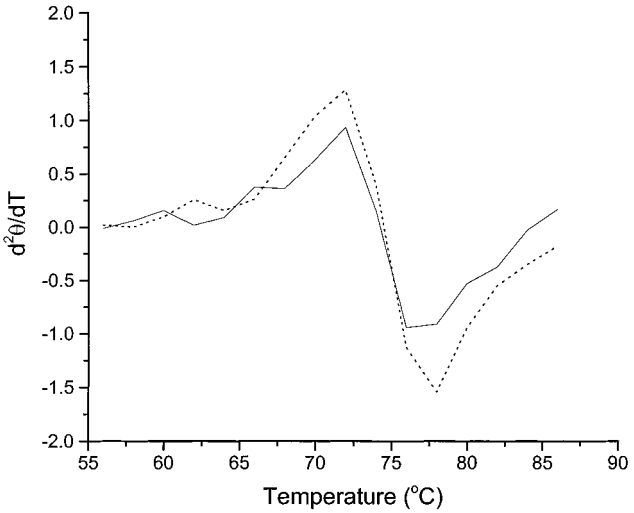

FIGURE 2: Second derivative of the temperature dependence of the ellipticity of u-Mb (—) and t-Mb (···). CD measurements of the carbonmoxy derivatives were taken at 225 nm over a range of temperature. Protein concentration was 1×10^{-5} M in 20 mM phosphate buffer at pH 7.8.

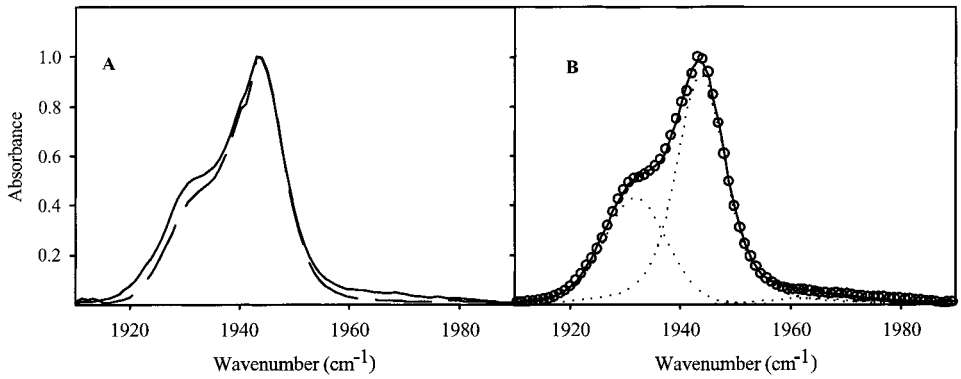

FIGURE 3: FTIR spectra of myoglobins. (A) Spectra at room temperature of the carbonmonoxy derivatives of u-Mb (—) and t-Mb (– –). (B) Fitting of the u-Mb spectrum in terms of Voigtian components. Experimental data (○) are shown with the Voigtian components (•••) and the overall calculated band profile (—).

Table 1: Fluorescence Lifetimes of Recombinant Myoglobins[a]

	α_1 (%)	τ_1 (ps)	α_2 (%)	τ_2 (ps)	α_3 (%)	τ_3 (ps)	α_4 (%)	τ_4 (ps)
u-Mb	55 (9.3)	25	42 (36.7)	129	2 (20.4)	1504	1 (33.6)	4953
t-Mb	60 (11.7)	25	38 (38.0)	129	1 (11.7)	1504	1 (38.5)	4953

[a] The fluorescence lifetime (τ), relative amplitude (α), and fractional intensity (in parentheses) were determined for untreated (u-Mb) and treated (t-Mb) recombinant myoglobins.

ponent τ_4 at about 5 ns has been assigned to a myoglobin fraction with reversibly dissociated hemes.

FTIR Spectroscopy. We measured the FTIR absorption spectra of the CO derivatives, to compare the electrostatic environment around bound ligands in u-Mb and t-Mb (Figure 3). We applied a standard approach (*47*) to fit these spectra in terms of three Voigtian components which correspond to the three taxonomic conformational substates A_0 ($\nu_{CO} \approx 1964$ cm^{-1}), A_1 ($\nu_{CO} \approx 1944$ cm^{-1}), and A_3 ($\nu_{CO} \approx 1932$ cm^{-1}). The parameter values obtained by this analysis (peak frequencies, half-widths at half-maximum, areas as percent of the total) are reported in Table 2. The raw spectra in Figure 3 point to an altered distribution of the A substates in u-Mb relative to that of Mb and t-Mb. This is confirmed by the spectral analysis showing that in u-Mb the relative distribution of the substates is modified, with A_1 being 64% of the total, as compared to 71 and 70% in Mb and t-Mb, respectively, and A_3 being 33% of the total, as compared to 25 and 28% in Mb and t-Mb, respectively. A line width increase is also observed for A_3 in u-Mb while the other parameters remain unaffected. Thus, similar to the CD results, the FTIR absorption spectra of Mb and t-Mb are indistinguishable after the acidic oxidation−reduction treatment.

Optical Absorption Spectroscopy. The Soret bands of unliganded and carbonmonoxy Mb at various temperatures and their deconvolutions in terms of eq 2 have been previously reported (*48*, *49*). The spectra of the u-Mb and t-Mb proteins (both CO and deoxy derivatives) are very similar to those of Mb and are therefore not presented.

From analysis of the spectra measured at various temperatures, we extracted the following information:

(a) Vibrational coupling with "high frequency" modes (parameters S_i), lifetime of the excited state (parameter Γ), homogeneous broadening related to the lifetime of the excited states ($Q_0\sqrt{b}$ and $\delta\sqrt{b}$). The values of these parameters are essentially the same in all the investigated proteins (*18*, *48*, *49*).

(b) Temperature dependence of the peak frequency of the Soret band (parameter ν_0). This is presented in Figure 4. For u-Mb, a blue shift of about 50 cm^{-1} for the CO derivative and of about 25 cm^{-1} for the deoxy derivative was observed. However, the temperature dependence of ν_0 was similar for both derivatives. In addition, the magnitude of this shift was not temperature-dependent. Moreover, for both derivatives, the blue shift was abolished by the acidic oxidation−reduction treatment.

(c) Temperature dependence of the Gaussian width of the band (parameter σ^2). Figure 5 shows that larger σ^2 values were observed for both derivatives of u-Mb; however, the temperature dependence was similar. The continuous lines represent fits of the σ^2 temperature dependence in terms of the harmonic Einstein model; in Table 3 we report the values of the parameters, obtained from the fits, that describe the coupling with the Einstein bath of low-frequency modes. Consistent with the unaffected temperature dependence, neither the average frequency of the bath (parameter $\langle\nu\rangle$) nor the average coupling constant (parameter *NS*) was affected. However, for both derivatives, u-Mb exhibited larger values of σ_{in}, which reflects greater spectral and conformational heterogeneity. The acidic oxidation−reduction treatment restored small F_{in} values, reflecting reduced heterogeneity.

(d) Anharmonicity. As shown in Figure 5, the harmonic behavior is observed only at low temperatures. In Figure 6 we present the anharmonic contributions as a function of temperature (parameter $\Delta\sigma^2$, i.e., the difference between the observed σ^2 values and the predictions of the harmonic model). The difference among the three proteins, if any, is very small. Although data referring to both derivatives of u-Mb systematically appear above those of Mb and t-Mb, the differences are not significant as they are at the limits of the experimental error.

Kinetics of CO Binding. To investigate the functional relevance of the spectral alterations reported above, we examined the kinetics of CO binding after flash-photolysis. Figure 7 shows typical time courses for u-Mb and t-Mb. The data were first analyzed using a multiexponential model. The CO binding curve of t-Mb was fit by a single major component (94% of total), although a minor component was observed (6% of total). In contrast, the CO binding curve of u-Mb was fit by two components of similar amplitudes whose

Table 2: Parameters of the A Substates Obtained by Fitting the Spectra in Figure 2 with Voigtian Components[a]

	I_{A0} (%)	ν_{A0} (cm^{-1})	WHM_{A0} (cm^{-1})	I_{A1} (%)	ν_{A1} (cm^{-1})	WHM_{A1} (cm^{-1})	I_{A3} (%)	ν_{A3} (cm^{-1})	WHM_{A3} (cm^{-1})
Mb-CO	4 ± 1	1963.4 ± 0.5	15 ± 3	71 ± 1	1944.1 ± 0.4	12.0 ± 0.8	25 ± 1	1931.6 ± 0.4	12.2 ± 0.4
u-Mb-CO	3 ± 1	1963.2 ± 0.5	18 ± 4	64 ± 1	1943.8 ± 0.4	11 ± 0.6	33 ± 1	1931.8 ± 0.4	13.6 ± 0.2
t-Mb-CO	2 ± 1	1963.7 ± 0.5	18 ± 5	70 ± 1	1943.8 ± 0.4	11 ± 0.6	28 ± 1	1931.9 ± 0.5	11.8 ± 0.2

[a] Errors refer to 90% confidence intervals. Mb-CO data were taken from ref *63*.

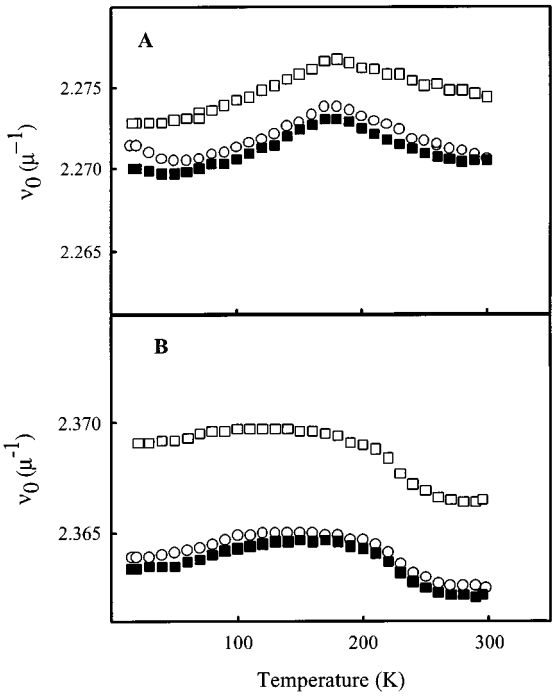

FIGURE 4: Temperature dependence of the peak frequency of the Soret band. The temperature dependence of the parameter ν_0 is shown for deoxy (A) and carbonmonoxy (B) derivatives of Mb (○), u-Mb (□), and t-Mb (■).

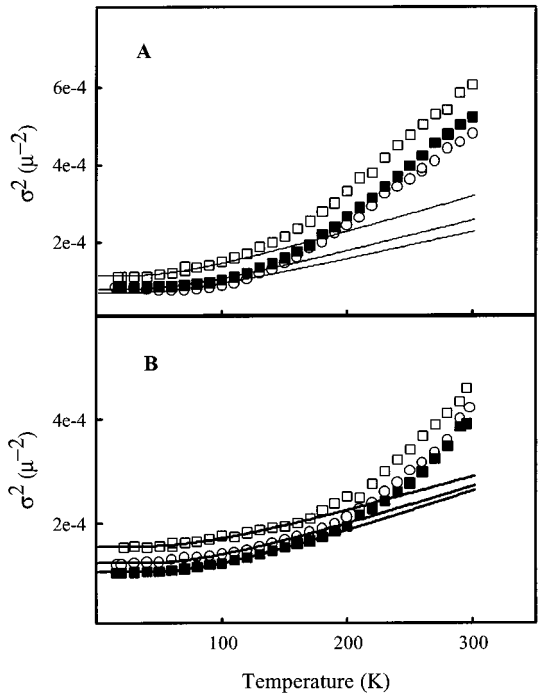

FIGURE 5: Temperature dependence of parameter σ^2. Panels and symbols as in Figure 4. The solid lines represent fittings of the low-temperature data in terms of the harmonic model (eq 2).

Table 3: Values of the Parameters Obtained by Fitting the Low-Temperature σ^2 Behavior with Equation 2

	NS	$\langle\nu\rangle$ (cm^{-1})[a]	σ_{in}
Mb	0.45 ± 0.1	132	0 ± 10
u-Mb	0.5 ± 0.1	132	50 ± 10
t-Mb	0.45 ± 0.1	132	0 ± 10
Mb-CO	0.3 ± 0.1	180	45 ± 5
u-Mb-CO	0.3 ± 0.1	180	82 ± 5
t-Mb-CO	0.3 ± 0.1	180	12 ± 8

[a] To avoid fitting ambiguities, the values of $\langle\nu\rangle$ were kept constant in the fittings.

rates varied about 2-fold (see Table 4). The data were also analyzed in terms of distributions of exponentials (i.e., distributions of binding rate constants) using the maximum entropy method (MEM), a statistical approach that has previously been applied to yield fine details of heme protein dynamics (*50*, *51*). The results of MEM analysis (Figure 8) show that the kinetics of CO binding to u-Mb are best described by a broad, bimodal distribution (Figure 8B). Conversely, after the acidic oxidation−reduction treatment, the distribution becomes very narrow with a peak at a slightly higher log k value (Figure 8A). The small fraction (about 5%) observed at log $k = 1.8$ for t-Mb (and also in the standard exponential fit) may be attributed to a small fraction of damaged protein.

DISCUSSION

For this investigation, we sought to construct an *E. coli* expression system for myoglobin in which the N-terminal methionine initiator was removed in vivo. Although the resulting level of myoglobin expression was good, protein sequencing indicated that the cleavage of the amino-terminal residues extended five or more residues past the N-terminal methionine. This problem was not observed by Shen et al. (*27*) in recombinant hemoglobin obtained with a similar expression system. This discrepancy most probably arises from differences in the sequence of the N-terminal residues in the A helices of human Hb and sperm whale Mb. Consequently, for this work we selected growth conditions in which more than 95% of the expressed myoglobin retained the initiator methionine.

Several types of spectroscopic approaches consistently suggest that the expressed myoglobin has a distorted (i.e., non-native) heme pocket conformation. The presence of an altered heme pocket conformation in the expressed u-Mb is indicated by modifications of the Soret CD spectrum (Figure 1), the FTIR spectrum and distribution of A substates (Figure 3), a blue shift of the peak frequency of the Soret band (Figure 4), and the larger widths of the absorption bands (Figure 5 and Tables 2 and 3). This conformational modification is reflected in altered functionality, as the CO binding kinetics of u-Mb are best described by two rate constants of similar amplitude (Table 4). MEM analysis of the same data

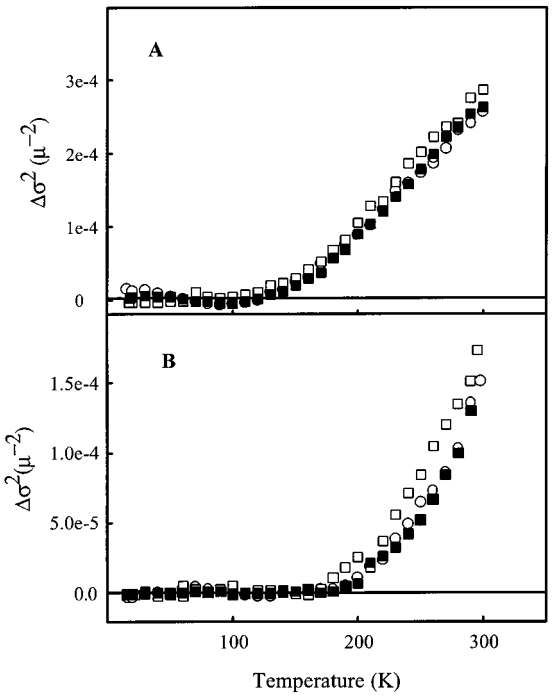

FIGURE 6: $\Delta\sigma^2$ values as a function of temperature. Panels and symbols as in Figures 4 and 5.

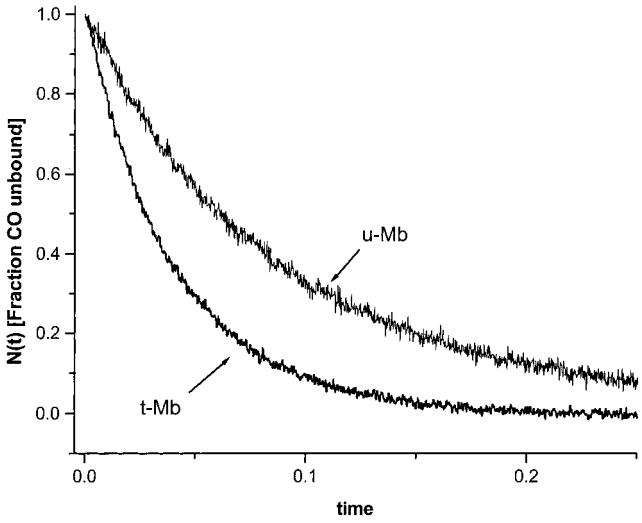

FIGURE 7: Kinetics of CO binding to myoglobins following flash photolysis. The time course for disappearance of CO-free u-Mb and t-Mb is shown. Protein concentration was 5×10^{-6} M in 0.1 M Bis-Tris, 0.1 M KCl (pH 7.0) at 20 °C.

Table 4: Kinetic Parameters of CO Binding to Myoglobins[a]

	α[b]	k (μM^{-1} s^{-1})
u-Mb	0.58 ± 0.09	0.19 ± 0.03
	0.42 ± 0.09	0.38 ± 0.05
t-Mb	0.94 ± 0.03	0.50 ± 0.05
	0.06 ± 0.03	1.78 ± 0.66

[a] The fractional amount (α) and CO binding rate constant (k) were determined for untreated (u-Mb) and treated (t-Mb) recombinant myoglobins, based on multiexponential analyses of the kinetic data in Figure 7. [b] Fractional content of component calculated from absorbances (eq 5).

similarly indicates a wide, bimodal, distribution of substates with different CO binding rates (Figure 8). Fluorescence measurements (Table 1) indicate that the amount of 180° inverted hemes is very small, 1−2% in both u-Mb and t-Mb;

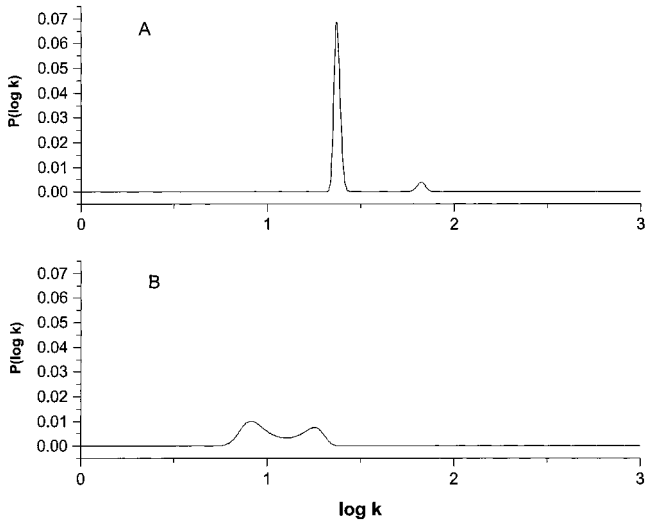

FIGURE 8: Rate distribution of CO binding to myoglobin. MEM analysis of the data in Figure 7 yielded the rate profiles for t-Mb (A) and u-Mb (B). The distribution shows the calculated probability (P) for the range of CO binding rate (log k).

therefore, the observed spectroscopic effects cannot be attributed to molecules with inverted heme. This is consistent with a report that subtle modifications of the heme pocket, not attributable to inverted heme, were observed with NMR measurements of reconstituted human hemoglobin produced by in vitro reassembly of *E. coli*-expressed α-globin with heme and native β-globin (*42*).

In view of the highly symmetric structure of the porphyrin, the origin of the heme Cotton effect in myoglobin has been attributed to heme−protein interactions and in particular to coupled oscillator interactions between the heme transitions and allowed $\pi \rightarrow \pi^*$ transitions in nearby aromatic side chains (*52*). The altered heme pocket conformation, therefore, must involve the aromatic residues within and/or near the heme pocket: the proximal and distal histidines, together with the phenylalanines at the C−D corner and the histidine at the F−G corner, are the most plausible candidates.

On the other hand, the blue shift of the Soret band (Figure 4), observed for both liganded and deoxy derivatives at all temperatures, is indicative of an altered local electric field at the heme chromophore (*33*) in u-Mb. This is in agreement with data from FTIR spectroscopy showing altered populations of the A substates and, therefore, an altered electrostatic environment for the bound CO molecule (*17*, *53*). In particular, the decrease of the A_1 substate with a concomitant increase of the A_3 substate (see Table 2) strongly supports the involvement of the proximal histidine at position F8 (*54*) in the altered heme pocket observed in u-Mb. This is consistent with stabilization of the F helix as the last step of the heme pocket refolding in Mb (*3*, *25*).

The larger widths consistently observed not only for the spectral bands (Soret-CD, Soret-absorption, and IR) but also for the distribution of rate constants for CO binding strongly suggest that the partially incorrect heme pocket folding in u-Mb protein reflects an increased conformational heterogeneity, i.e., a wider distribution of protein conformational substates (*33*). The temperature dependence of the Soret band indicates that the overall dynamic properties of the heme pocket, and the coupling of the heme electronic transition with the bath of low-frequency modes of the heme−protein

system, are not substantially altered; the slight increase in anharmonicity suggested by the $\Delta\sigma^2$ values in Figure 6 would be consistent with an increase of anharmonic motions in the partially incorrectly folded conformation.

The CO binding kinetics data are fully consistent with the spectroscopic data, in that they reveal that the kinetic profile of u-Mb is characterized by a wider distribution of rate constants, which implies a wider distribution of enthalpy barriers for the binding of CO to the heme (*55*). This increased conformational heterogeneity indicates an increased number of noninterconverting conformational substates at room temperature, in the time scale of the CO binding reaction. The data also show that the partially incorrect folding of the heme pocket in u-Mb has functional relevance, dereasing, on the average, the rate of ligand recombination. This is evidenced by a rate distribution for u-Mb (Figure 8) which, besides its larger width, is centered around lower *k* values than that of t-Mb. The acidic oxidation−reduction treatment resulted in a complete conversion of the spectroscopic properties of the expressed u-Mb to those of Mb, therefore restoring a nativelike heme pocket conformation. The non-native CO binding kinetics of u-Mb differ from those previously reported for *E. coli* expressed sperm whale Mb which exhibited a rate and homogeneity similar to native Mb (*14*). Since the functional characteristics are not altered in Mb preparations containing inverted heme (*56*, *57*), we do not attribute the altered functionality of u-Mb to the presence of inverted heme. This is supported by the fluorescence data that indicate a minimal amount of inverted heme in our sample. It should be noted that the altered folding of u-Mb is limited to the heme pocket and does not affect the overall tertiary and secondary structure of the protein. This is indicated by the similar fluorescence lifetimes of tryptophans 7 and 14 in u-Mb and t-Mb (Table 1), by the similar resistance to thermal denaturation (respective T_m values of 74.5 and 74.3 °C) (Figure 2), and by the same helical content (data not shown).

The incorrect heme pocket refolding reported here is probably confined to Mb refolded in vivo in microorganisms. It could also be specific to our Mb expression system, since a recombinant Mb obtained using a different expression system without the acidic oxidation−reduction treatment had the same rate of CO binding as natural sperm whale Mb (*14*). Transient modifications of the heme pocket conformation have been observed in measurements carried out using native sperm whale apomyoglobin reconstituted with heme in vitro. They have been attributed to two interconverting protein forms at equilibrium in solution, which differ by a reorientation of the heme by a 180° rotation about the $\alpha-\gamma$ meso axis (*56*, *58*, *59*). These conformers have similar ligand affinity (*56*, *57*). 2D NMR measurements of recombinant human Mb did not detect conformational modifications of the heme pocket (*60*). This protein was expressed as fusion protein and reconstituted in vitro with heme. In these measurements, the conformational modifications of the heme pocket observed for a number of heme pocket mutant human Mb's were also minor, although the functional characteristics of those Mb's were modified. The sensitivity of 2D NMR may not be sufficient for discriminating between conformers carrying subtle conformational changes.

Folding of the heme pocket of Mb is the last step in attaining the native structure, and occurs only upon binding of the heme (*3*, *5*, *9*, *10*). In the recombinant u-Mb, the synchrony between correct heme pocket refolding and heme binding is disrupted, and the globin chain folds around the heme in a heterogeneous, partially incorrect (i.e., non-native) conformation. The resulting protein molecules are then confined within a given subset of conformational substates whose spectroscopic and functional properties differ from those of Mb. In the ferric form at acid pH, the affinity for the heme is decreased, and the heme pocket is capable of sampling additional conformations in a "soft unfolding" process. This increased conformational flexibility allows the protein to search different conformations and eventually adopt one that corresponds to that of the native heme pocket. In more physical terms, the acidic oxidation−reduction treatment allows the protein to explore a larger portion of the conformational space; this "annealing" process enables the protein to achieve its correct minimum energy configuration on a highly rugged energy landscape (*61*, *62*).

In the absence of an experimental structure for our protein, the amino acid residue(s) that contribute(s) to the acid-induced soft unfolding of u-Mb cannot be positively identified. However, spectroscopic studies of acid-induced denaturation of various forms of Mb (*64*−*67* and references cited therein) have defined the role of specific helical regions and some residues in the unfolding and refolding process. Although stronger acidic conditions were employed (less than pH 3.5 whereas we used pH 5.3), results of these previous studies can nevertheless be used to suggest candidates responsible for the acid-sensitivity of u-Mb. The most likely residues are the proximal and distal histidines. Protonation of the proximal His93 would disrupt the coordinate Fe−His linkage and significantly disrupt structure of the heme region. Protonation of the distal His64 in its hydrophobic environment would likewise be expected to destabilize the heme region and facilitate conformational flexibility. Since NMR studies (*68*, *69*) show a higher p*K* for the distal His64, its higher degree of protonation at pH 5.3 suggests this residue as the more likely contributor to heme pocket destabilization.

Besides these histidines, acid-induced rearrangements of other structural segments can destabilize the heme region. Several spectroscopic probes were used to study acid-induced unfolding and subsequent refolding of CO-myoglobin encapsulated in a sol−gel matrix to slow these processes and allow for observation of folding intermediates (*67*). The most acid-sensitive region was found to be the A helix, whose initial disruption leads to subsequent destabilization of other regions. Among the observed pH-folding intermediates were species with a distorted Fe−His linkage, and with water as a strong heme ligand. With a partially unfolded A helix, the stability of the latter is similar to that of the intact myoglobin at neutral pH. Thus, two species with different heme pocket configurations coexist and are separated by a kinetic barrier. A similar situation may exist for our expressed u-Mb in which multiple species are kinetically trapped in various conformations, and may interconvert with mild acid denaturation at pH 5.3.

These data indicate that the final step of Mb refolding in vivo requires a precise intercorrelation between the rate of protein synthesis, folding, and heme binding. When this synchronism is altered, the heme pocket does not attain its final native structure. The nature of the factors altering the

correct synchronism of the processes involved in the in vivo heme pocket refolding, is, at present, not well-defined.

ACKNOWLEDGMENT

The technical help of Mr. G. Lapis of the cryogenic laboratory in Palermo is gratefully acknowledged.

REFERENCES

1. Jennings, P. A., and Wright (1993) *Science 262*, 892−896.
2. Hughson, F. M., and Baldwing, R. L. (1989) *Biochemistry 28*, 4415−4422.
3. Eliezer, D., and Wright, P. E. (1996) *J. Mol. Biol. 263*, 531−538.
4. Roder, H., Elove, G. A., and Englander, S. W. (1988) *Nature 335*, 700−704.
5. Griko, Y. V., Privalov, P. L., Venyaminov, S. Y., and Kutyshenko, V. P. (1988) *J. Mol. Biol. 202*, 127−138.
6. Yip, Y. K., Waks, M., and Beychok, S. (1973) *J. Biol. Chem. 247*, 7237.
7. Fronticelli and Bucci (1975) *Biochemistry 14*, 4451−4458.
8. Franchi, D., Fronticelli, C., and Bucci, E. (1982) *Biochemistry 21*, 6181−6187.
9. Hargrove, M. S., Barrick, D., and Olson, J. S. (1996) *Biochemistry 35*, 11300−11309.
10. Hargrove, M. S., and Olson, J. S. (1996) *Biochemistry 35*, 11310−11318.
11. Egeberg, K. D., Springer, B. A., Sligar, S. G., Carver, T. E., Rohlfs, R. J., and Olson, J. S. (1990) *J. Biol. Chem. 265*, 11788−11795.
12. Whitaker, T. L., Berry, M. B., Emai, L. H., Hargrove, M. S., Phillips, G. N., Komiyama, N. H., Nagai, K., and Olson, J. S. (1995) *Biochemistry 34*, 8221−8226.
13. Uchida, T., Ishimori, K., and Morishima, I. (1997) *J. Biol. Chem. 272*, 30108−30114.
14. Springer, B. A., Sligar, S. G., Olson, J. S., and Phillips, G. N. (1994) *Chem. Rev. 94*, 699−714.
15. Sirangelo, I., Tavassi, S., Martelli, P. L., Casadio, R., and Irace, G. (2000) *Eur. J. Biochem. 267*, 3937−3945.
16. Fronticelli, C., Sanna, M. T., Perez-Alvarado, G. C., Karavitis, M., Lu, A.-L., and Brinigar, W. S. (1995) *J. Biol. Chem. 279*, 30588−30592.
17. Cupane, A., Leone, M., Militello, V., Friedman, F. K., Koley, A. P., Vasquez, G. B., Brinigar, W. S., Karavitis, M., and Fronticelli, C. (1997) *J. Biol. Chem. 272*, 26271−26278.
18. Karavitis, M., Fronticelli, C., Brinigar, W. S., Vasquez, G. B., Militello, V., Leone, M., and Cupane, A. (1998) *J. Biol. Chem. 273*, 23740−23749.
19. Chen, W., Dumoulin, A., Li, X., Padovan, J. C., Chait, B. T., Buonopane, R., Platts, O. S., Manning, L. R., and Manning, J. M. (2000) *Biochemistry 39*, 3774−3781.
20. Barrick, D., Ho, N. T., Simplaceanu, V., Dalquist, F. W., and Ho, C. (1997) *Nat. Struct. Biol. 4*, 78−83.
21. Brunori, M., Vallone, B., Cutruzzola', F., Travaglini-Allocatelli, C., Berendzen, J., Chu, K., Sweet, R. M., and Schlichting, I. (2000) *Proc. Natl. Acad. Sci. U.S.A. 97*, 2058−2063.
22. Acampora, G., and Hermans, J., Jr. (1967) *J. Am. Chem. Soc. 89*, 1543−1547.
23. Hughson, F. M., Wright, P. E., and Baldwin, R.l. (1990) *Science 249*, 1544−1548.
24. Tang, Q., Kalsbeck, W. A., Olson, J. S., and Bocian, D. F. (1998) *Biochemistry 37*, 7047−7056.
25. Lecomte, J. T. J., Sukists, S. S., Bhattacharya, S., and Falzone, C. J. (1999) *Protein Sci. 8*, 1484−1491.
26. Springer, B. A., and Sligar, S. G. (1987) *Proc. Natl. Acad. Sci. U.S.A. 84*, 8961−8965.
27. Shen, T.-J., Ho, N. T., Simplaceanu, V., Zou, M., Green, B. N., Tam, M. F., and Ho, C. (1993) *Proc. Natl. Acad. Sci. U.S.A. 90*, 8108−8112.
28. Laczko, G. I., Gryczynski, I., Gryczynski, Z., Wiczk, W., Malak, H., and Lakowicz, J. R. (1990) *Sci. Instrum. 61*, 2331−2337.
29. Gryczynski, K., and Bucci, E. (1993) *Biophys. Chem. 48*, 31−38.
30. Gryczynski, K., Beretta, S., Lubkowski, J., Razynska, A., Gryczynski, I., and Bucci, E. (1997) *Biophys. Chem. 64*, 81−91.
31. Gryczynski, Z., and Bucci, E. (1998) *Biophys. Chem. 74*, 187−189.
32. Cupane, A., Leone, M., Vitrano, E., and Cordone, L (1995) *Eur. Biophys. J. 23*, 385−398.
33. Frauenfelder, H., Parak, F., and Young, R. D. (1988) *Annu. Rev. Biophys. Chem. 17*, 451−479.
34. Markowitz, A., Robinson, R. C., Omata, Y., and Friedman, F. K. (1992) *Anal. Instrum. 20*, 213−221.
35. Koley, A. P., Robinson, R. C., Markowitz, A., and Friedman, F. K. (1995) *Biochemistry 34*, 1942−1947.
36. Koley, A. P., Buters, J. T. M., Robinson, R. C., Markowitz, A., and Friedman, F. K. (1995) *J. Biol. Chem. 270*, 5014−5018.
37. Koley, A. P., Robinson, R. C., and Friedman, F. K. (1996) *Biochimie 78*, 706−713.
38. Koley, A. P., Robinson, R. C., Markowitz, A., and Friedman, F. K. (1996) *Arch. Biochem. Biophys. 336*, 261−267.
39. Koley, A. P., Dai, R., Robinson, R. C., Markowitz, A., and Friedman, F. K. (1997) *Biochemistry 36*, 3237−3241.
40. Koley, A. P., Buters, J. T. M., Robinson, R. C., Markowitz, A., and Friedman, F. K. (1997) *J. Biol. Chem. 272*, 3149−3153.
41. Smith, S. V., Koley, A. P., Dai, R., Robinson, R. C., Leong, H., Markowitz, A., and Friedman, F. K. (2000) *Biochemistry 39*, 5731−5737.
42. Sanna, M. T., Razynska, A., Karavitis, M., Koley, A. P., Friedman, F. K., Russu, I. M., and Fronticelli, C. (1997) *J. Biol. Chem. 272*, 3478−3486.
43. La Mar, G. N., Toi, H., and Krishnamoorthi (1984) *J. Am. Chem. Soc. 106*, 6395−6401.
44. Ajoula, H. S., Wilson, M. T., and Drake, A. (1986) *Biochem. J. 237*, 613−616.
45. Gryczynski, Z., Lubkowski, J., and Bucci, E. (1997) *Methods Enzymol. 278*, 538−569.
46. Gryczynski, Z., Lubkowski, J., and Bucci, E. (1995) *J. Biol. Chem. 270*, 19232−19237.
47. Alben, J. O., Beece, D., Bowne, S. F., Doster, L., Eisenstein, L., Frauenfelder, H., Good, D., McDonald, J. D., Marden, M. C., Moh, P. P., Reinisch, A. H., Shyamsunder, E., and Yue, K. T. (1982) *Proc. Natl. Acad. Sci. U.S.A. 79*, 3744−3748.
48. Di Pace, A., Cupane, A., Leone, M., Vitrano, E., and Cordone, L. (1992) *Biophys. J. 63*, 475−484.
49. Cupane, A., Leone, M., Vitrano, E., Cordone, L., Hiltpold, U. R., Winterhalter, K. H., Yu, W., and Di Iorio, E. E. (1993) *Biophys. J. 65*, 2461−2472.
50. Steinbach, P. J. (1996) *Biophys. J. 70*, 1521−1528.
51. Johnson, J. B., Lamb, D. C., Frauenfelder, H., Muller, J. D., McMahon, B., Nienhaus, G. U., and Young, R. D. (1996) *Biophys. J. 70*, 1563−1573.
52. Hsu, M.-C., and Woody, R. W. (1971) *J. Am. Chem. Soc. 93*, 3515−3525.
53. Li, X. Y., and Spiro, T. (1988) *J. Am. Chem. Soc. 110*, 6024−6033.
54. Vojtechovsky, J., Chu, K., Berendzen, J., Sweet, R. M., and Schlichting, I. (1999) *Biophys. J. 77*, 2153−2174.
55. Ansari, A., Di Iorio, E. E., Dlott, D. D., Frauenfelder, H., Iben, I. E. T., Langer, P., Roder, H., Sauke, T. B., and Shyamsunder, E. (1986) *Biochemistry 25*, 3139−3146.
56. Light, W. R., Rohlfs, R. J., Palmer, G., and Olson, J. S. (1987) *J. Biol. Chem. 262*, 46−52.
57. Aojoula, H. S., Wilson, M. T., and Morrison, I. E. G. (1987) *Biochem. J. 243*, 205−210.
58. La Mar, G. N., Davis, N. L., Pariush, D. W., and Smith, K. M. (1983) *J. Mol. Biol. 168*, 887−896.
59. Aojoula, H. S., Wilson, M. T., and Drake, A. (1986) *Biochem. J. 237*, 613−616.

60. Varadarajan, R., Lambright, D. G., and Boxer, S. G. (1989) *Biochemistry 28*, 3771−3778.
61. Dill, K. A., and Chan, H. S (1997) *Nat. Struct. Biol. 4*, 10−19.
62. Frauenfelder, H., and Wolynes, P. G. (1994) *Phys. Today 47*, 58−64.
63. Librizzi, F., Vitrano, E., and Cordone, L. (1999) *Biophys. J. 76*, 2727−2734.
64. Konerman, L., Rosell, F. I., Mauk, A. G., and Douglas, D. J. (1997) *Biochemistry 36*, 6448−6454.
65. Chi, Z., and Asher, S. (1998) *Biochemistry 37*, 2865−2872.
66. Tang, Q., Kalsbeck, W. A., Olson, J. S., and Bocian, D. F. (1998) *Biochemistry 37*, 7047−7056.
67. Samuni, U., Navati, M. S., Juszczak, L. J., Dantsker, D., Yang, M., and Friedman, J. M. (2000) *J. Phys. Chem. 1047*, 10802−10813.
68. Lecomte, J. T., and La Mar, G. N. (1985) *Biochemistry 24*, 7388−7395.
69. Osapay, K., Theriault, Y., Wright, P. E., and Case, D. A. (1994) *J. Mol. Biol. 244*, 183−197.

BI010652F